Direct observations of rock moisture, a hidden component of the hydrologic cycle

Daniella M. Rempe[a,1] and William E. Dietrich[b,1]

[a]Department of Geological Sciences, Jackson School of Geosciences, University of Texas at Austin, Austin, TX 78701; and [b]Department of Earth and Planetary Science, University of California, Berkeley, CA 94720

Contributed by William E. Dietrich, January 30, 2018 (sent for review January 4, 2018; reviewed by John R. Nimmo and Ying Fan)

Recent theory and field observations suggest that a systematically varying weathering zone, that can be tens of meters thick, commonly develops in the bedrock underlying hillslopes. Weathering turns otherwise poorly conductive bedrock into a dynamic water storage reservoir. Infiltrating precipitation typically will pass through unsaturated weathered bedrock before reaching groundwater and running off to streams. This invisible and difficult to access unsaturated zone is virtually unexplored compared with the surface soil mantle. We have proposed the term "rock moisture" to describe the exchangeable water stored in the unsaturated zone in weathered bedrock, purposely choosing a term parallel to, but distinct from, soil moisture, because weathered bedrock is a distinctly different material that is distributed across landscapes independently of soil thickness. Here, we report a multiyear intensive campaign of quantifying rock moisture across a hillslope underlain by a thick weathered bedrock zone using repeat neutron probe measurements in a suite of boreholes. Rock moisture storage accumulates in the wet season, reaches a characteristic upper value, and rapidly passes any additional rainfall downward to groundwater. Hence, rock moisture storage mediates the initiation and magnitude of recharge and runoff. In the dry season, rock moisture storage is gradually depleted by trees for transpiration, leading to a common lower value at the end of the dry season. Up to 27% of the annual rainfall is seasonally stored as rock moisture. Significant rock moisture storage is likely common, and yet it is missing from hydrologic and land-surface models used to predict regional and global climate.

Critical Zone | rock moisture | deep vadose zone | water budget | evapotranspiration

Transpiration, the return of water to the atmosphere by plants, likely greatly exceeds terrestrial evaporation and runoff, yet remains a key source of uncertainty in models of global climate that provide critical projections of Earth's water resources into the future (1, 2). With recent advances in satellite-based remote sensing observations (3) and the establishment of large-scale soil moisture-monitoring networks (4), the role of the soil layer in regulating evaporation and transpiration (evapotranspiration; ET) fluxes has received intensive study. There is growing recognition, however, that water supply for transpiration is often derived from depths deeper than the soil (5). For example, the use of groundwater by vegetation (either directly or by recharging soil moisture via upward capillary fluxes) has been directly incorporated into hydrologic and climate models (6, 7).

In soils developed on bedrock, the term soil typically refers to the physically mobile, granular surface mantle that lacks relict rock structure (Fig. 1). Intensive studies have directly demonstrated that the weathered bedrock that lies beneath soils may be a critical source of water to plants that is distinct from soil moisture or groundwater (8–10). Hydrologic studies also suggest that the timing and composition of streamflow (runoff) are influenced by the transit of infiltrating rainfall through meters of unsaturated weathered bedrock (11–13). Large areas of deeply weathered bedrock extend across regions straddling the tropics in a broad range of rock types and tectonic and climatic settings (14, 15). Thus, the weathered bedrock region that lies beneath the soil layer and above the groundwater table may play a key role in how rainfall is partitioned between ET and runoff at large scales. However, because of the inaccessibility of the weathered bedrock underlying hillslopes, this zone is virtually unmapped, and its hydrologic properties and dynamics are poorly known. The emergence of research on the Critical Zone (CZ), which extends from the vegetation canopy through the soil and weathered bedrock (Fig. 1) has brought this gap to light.

In this study, we directly investigate the hydrologic dynamics of weathered bedrock. We specifically focus on quantifying the exchangeable, dynamic water stored in the matrix and fractures of weathered bedrock, which we propose to call "rock moisture" (16) (Fig. 1). The term rock moisture is parallel to, but distinct from, soil moisture. Soil moisture and rock moisture are expected to influence the hydrologic cycle in distinctly different ways, because both the properties and thickness of weathered bedrock vary independently from that of soil. While soil moisture dynamics have been measured at the pore to global scale (3), very few direct observations of rock moisture exist (17), and, therefore, incorporation of rock moisture dynamics into climate and hydrologic models remains challenging.

Here, we report the results of intensive mapping and long-term monitoring of rock moisture from the base of the soil to the groundwater table across a seasonally dry, forested hillslope in northern California. The site receives ~2,042 mm of precipitation annually (*Materials and Methods*), and previous studies have characterized a weathering profile developed in dense argillaceous bedrock that thickens upslope from 4 m near the channel to 25 m at the divide (Fig. 1) (16, 18). Thin (30–75 cm thick) soils overlie up to 4 m of saprolite (soil-like weathered rock that maintains the structure of the parent rock), and up to 20 m of weathered bedrock

Significance

Soil moisture has long been recognized as a key component of the hydrologic cycle. Here, we quantify significant exchangeable water held in weathered bedrock, beneath the soil, that regulates plant-available water and streamflow. We refer to this as rock moisture—a term parallel to soil moisture, but applied to different material. Deep weathered bedrock capable of storing plant-available moisture is common, yet this reservoir of rock moisture—distinct from soil and groundwater—is essentially unquantified. At our study site, the volume of rock moisture exceeds soil moisture and is a critical and stable source of water to plants in drought years. Our observations indicate that rock moisture now needs to be incorporated into hydrologic and climate models.

Author contributions: D.M.R. and W.E.D. designed research, performed research, analyzed data, and wrote the paper.

Reviewers: J.R.N., US Geological Survey; and Y.F., Rutgers University.

The authors declare no conflict of interest.

Data deposition: All data presented in this paper have been deposited at erczo.berkeley.edu/datasets under support-data-rempe-dietrich-pnas2018.zip.

[1]To whom correspondence may be addressed. Email: rempe@jsg.utexas.edu or bill@eps.berkeley.edu.

This article contains supporting information online at www.pnas.org/lookup/suppl/doi:10.1073/pnas.1800141115/-/DCSupplemental.

Published online February 28, 2018.

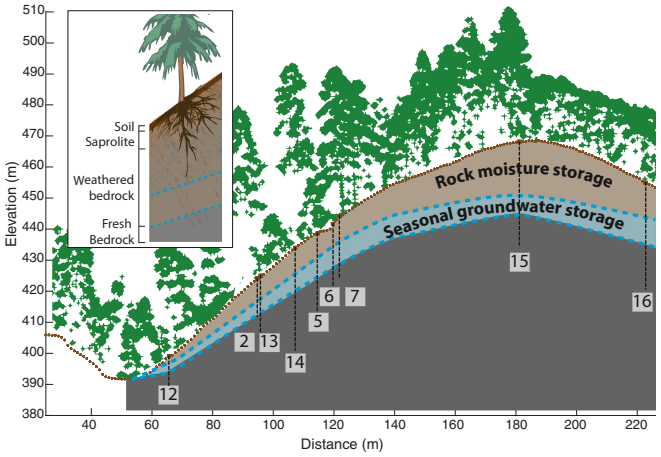

Fig. 1. Rock moisture storage within a hillslope: Cross-section of the study hillslope (latitude 39°43′44″N, longitude 123°38′39″W; Fig. S1) illustrating the Critical Zone structure, which extends from the tree canopy (green points reflecting lidar-derived canopy structure) to unweathered (i.e., fresh) bedrock (illustrated in dark gray). Well locations (vertical dashed lines) are projected onto the hillslope profile which extends across Elder Creek (Fig. S1). Three additional wells (wells 1, 3 and 10; shown in Fig. S1) were used to construct this weathering profile and hydrologic profile, but were not available for rock moisture monitoring. Rock moisture is stored between the base of the soil (soil thickness is similar to the scale of the brown dots denoting the ground surface) and the seasonally saturated zone, which is bounded by the minimum and maximum water table positions (approximate location derived from groundwater monitoring shown as blue dashed lines). In some cases, storage of rock moisture occurs below the seasonal maximum water table position. *Inset* is a conceptual vertical weathering profile illustrating thin soil overlying weathered bedrock which transitions to fresh bedrock at the base of the weathering profiles. (Lidar provided by the National Center for Airborne Laser Mapping.)

that shows decreasing fracturing and weathering with depth (Fig. 1, *Inset*) (18). No overland flow or runoff within soil or saprolite occurs at the site. Instead, infiltrating rainfall passes through the pervasively fractured weathered bedrock, collects on the underlying fresh bedrock boundary as groundwater, and flows laterally to the adjacent channel (16). In this study, we directly quantified rock moisture dynamics and identified its significance to the water budget using the intensive hydrologic monitoring infrastructure of the site and discrete neutron probe surveys made in boreholes across the site (*Materials and Methods*). Rock moisture storage, S (mm), was quantified as the depth-integrated change in rock moisture (i.e., volumetric water content) between the base of the soil and the groundwater table. The change in rock moisture was calculated relative to the driest, i.e., end-of-dry-season, condition (*Materials and Methods*).

A Seasonal Cycle of Rock Moisture Addition and Depletion Regulates Hydrologic Dynamics

In the Mediterranean climate of the study site, distinct wet and dry seasons permitted us to track a seasonal cycle of rock moisture addition and depletion, in which the weathered bedrock acts as a rock moisture "reservoir." At the conclusion of the dry season (October), the rock moisture reservoir was depleted to approximately the same level in different years (red lines in Fig. 2), despite large differences in the total volume of precipitation in the preceding wet season (precipitation before October 2015 and October 2016 was 1,359 and 2,168 mm, respectively; Table S1). In the earliest storms of the wet season, shallow soil moisture rose and fell with each storm, and there was progressive addition of rock moisture storage (Figs. 3 and 4*A*). As a wetting front advanced into the weathered bedrock, rock moisture storage progressively increased (Figs. 3*A* and 4*A*) and was roughly proportional to the corresponding cumulative seasonal precipitation at that time (Fig. 4*A*). In some wells, a small, short-lived groundwater response was observed (Fig. 3*C*) (16).

With continued precipitation, S increased until, each year, a similar seasonal maximum rock moisture storage (S_{max}) was reached at a given monitoring location (horizontal line in Fig. 4*A*). S_{max} at each well was consistent in different years and ranged between 100 and 550 mm among the different wells (Table S3). The average rock moisture S_{max} across all wells was 280 ± 140 mm (Table S3) and was 4.7 times the average soil moisture S_{max} across all measurement locations (Table S4). Despite year-to-year variability in the timing and magnitude of storms in the initial part of the wet season, the water table began to rise significantly at a given well only after nearly the same total volume of precipitation had fallen (denoted by red bands on abscissa in Fig. 4*A* and Table S2). This total precipitation at the time of significant well rise was roughly proportional to S_{max} (Fig. 4*A*).

The more extensive weathering of the bedrock near the ridge caused S_{max} to be the greatest there (550 and 350 mm in wells 15 and 16, respectively) (Fig. 4*A*). S_{max} decreased downslope from 170–330 mm midslope to 100 mm near the base of the hillslope, where the weathered bedrock zone was thinnest (Fig. 1 and Table S3). Groundwater response to the onset of the wet season initiated earlier in these wells relative to the wells located upslope, where the weathered bedrock zone was thicker (Fig. 3*C* and Table S2). Consequently, runoff dynamics were controlled by the mid and lower slope portions of the hillslope during the initial part of the wet season.

The additional rainfall that arrived after S_{max} was reached led to the relatively rapid response of the groundwater table to storms and the rapid delivery of groundwater to the stream as runoff (most likely by fracture flow) (16). The water table rose to varying heights within the weathered, fractured bedrock zone within hours to days of individual pulses of rain (Fig. 3*C*). The weathered bedrock within the water table fluctuation zone (denoted by light blue columns in Fig. 2) was likely persistently near saturation, because groundwater levels can rise by many meters in response to modest (<50 mm) storm events (Fig. 3*C*), and rock moisture showed only small changes at these depths. Between 46% and 70% of the total annual precipitation was delivered to the stream as runoff, and of that runoff, >80% occurred between October 1 and May 1 (Table S1). This left between 6 and 14 mm per month of baseflow for the final 2 months of the dry season (Table S1).

Throughout the long dry season, rock moisture slowly declined (Fig. 4*B*). Drying tended to initiate from the surface downward and progressed throughout the entire dry season (Fig. 3*B*). In contrast, soil moisture storage rapidly diminished following the last storm of the wet season (Fig. 3*C* and Fig. S2). In mid-June, when transpiration rates peaked across the site (19), between 50 and 403 mm of rock moisture storage was available, depending on hillslope position (Fig. 2 and Table S4). At this time, <25 mm of soil moisture storage remained (*SI Materials and Methods* and Table S4). Although the change in water content in the soil and weathered bedrock was comparable over the end of the dry season (Fig. 3 *B* and *C*), the greater thickness of the weathered bedrock zone led to much greater total rock moisture storage.

During the summer months, when transpiration is high (19), groundwater levels decline slowly, runoff is small, and large changes in rock moisture storage occur. Over 3 y of monitoring, the average dry-season rock moisture decline after mid-June ranged from 164 to 194 mm, whereas the corresponding runoff over that time was only 13 to 20 mm (Table S4). There is direct evidence of deep rooting at the site. We observed roots to 16 m depth in samples retrieved during drilling, and roots exposed in recent road cuts and the rootwads of fallen trees regularly show rooting directly into the deeper weathered bedrock below the depth of saprolite. We therefore hypothesize that the spatial pattern and magnitude of rock moisture depletion is controlled by rock moisture extraction by vegetation and that dry-season gravity drainage is minimal.

Dry-season rock moisture decline showed little year-to-year variability and no apparent sensitivity to the volume of precipitation that fell during the preceding wet season (Fig. 4*B* and Table S4). Even in a drought year of less than half mean annual precipitation (2014 received 1,027 mm of rain), the rock moisture storage capacity was reached, leading to the same pattern and

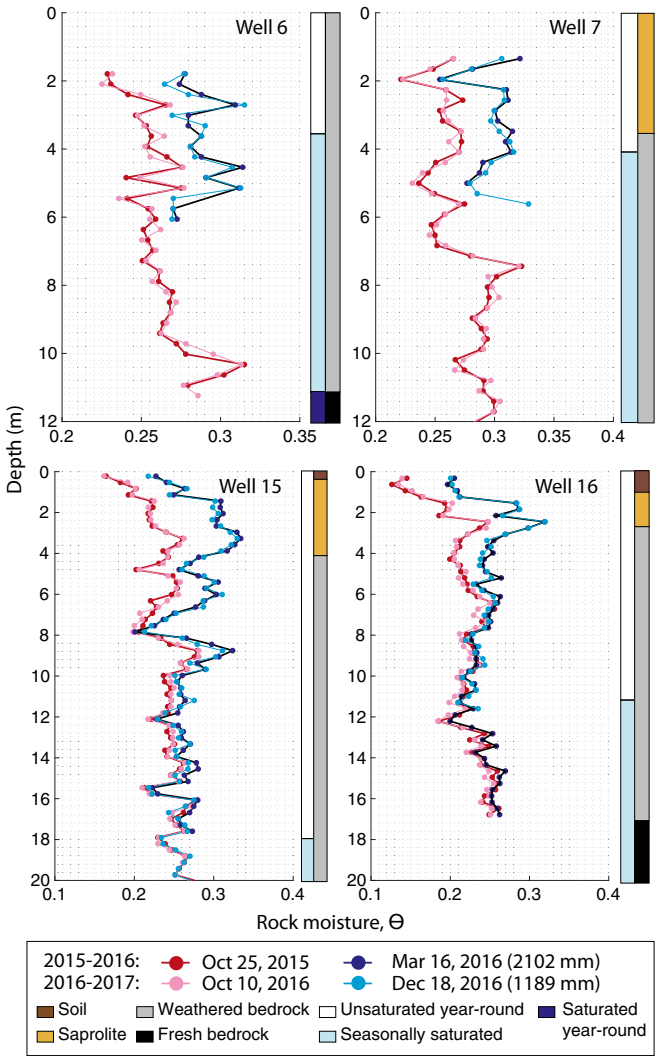

Fig. 2. A structured rock moisture reservoir: Vertical profiles of rock moisture expressed as volumetric water content, θ, in a subset of wells show that similar minimum (red) and maximum (blue) θ is reached in different years. Seasonal cumulative precipitation at the time of the wet-season measurement is shown in parentheses in the legend. Colored vertical bars on the right of each graph illustrate the zone of water table fluctuation identified via groundwater monitoring (left bars) and the weathering profile characteristics identified during drilling (right bars). Borehole locations are shown in Fig. 1 and Fig. S1.

magnitude of rock moisture depletion as years receiving more rainfall (1,359 mm in 2015 and 2,168 mm in 2016) (Fig. 4*B* and Table S4). Average dry-season rock moisture decline was 280 mm (Table S3). Hence, in 2016, when the site received approximately the mean annual precipitation, transpiration derived from rock moisture was up to 13% of the total precipitation, while in the dry year of 2014, it was up to 27% of total precipitation.

Discussion

Rock Moisture Dynamics: A Common Component of the Hydrologic Cycle. Our intensive, direct monitoring revealed the critical role of rock moisture storage to regulating the timing and magnitude of both runoff and ET fluxes. Significant storage of rock moisture and use by vegetation is likely common in a wide range of environments. A penetrating weathering front, which increases porosity and moisture storage potential in bedrock, is common in landscapes underlain by bedrock (20). Much of the slowly eroding, unglaciated cratons of the world have deep weathering profiles (14). Although arid environments are associated with lower rates of weathering and shallower weathering profiles, past climates often leave a legacy of extensive, deep weathering (15). Surprisingly, and consistent with theory (18, 21), even rapidly uplifting and eroding landscapes (such as the study site reported here) may be underlain by relatively deeply weathered bedrock, although it may not be strongly chemically altered (22). Thanks to heightened interest in modeling the evolution of the CZ (23), observations and theory (18, 24) are rapidly expanding our understanding of the structure of the weathered bedrock zone that underlies hillslopes. These approaches advance estimation of CZ depth and structure, which can lead to mapping of rock moisture storage potential across landscapes.

Contrary to long-standing assumptions, field studies are increasingly indicating that infiltration and lateral flow are not restricted to the soil layer (25–27). Unsaturated flow through, and storage within, weathered bedrock is common and has been explored via drilling (28), trenching (29), or tunneling (30) in a variety of geologic and climatic settings. Use of rock moisture by vegetation has been documented in diverse rock types with different styles of weathering—including the grus and matrix of weathered granites (31), within rough fractures and secondary clays in metasedimentary rocks (10), and cavernous, soil-filled voids in limestones (32)—suggesting that rock moisture storage is likely important in a variety of lithologic settings. Additionally, extraction of rock moisture by vegetation is documented not only in water-limited environments (32), but may play a key role in facilitating biogeochemical cycling in regions receiving ample rainfall (33). We propose, therefore, that rock moisture storage should be considered a common and potentially central component of the terrestrial hydrologic cycle.

Rock Moisture Mediates Biogeochemical Fluxes. Storage and circulation of rock moisture by plants influences water travel times within hillslopes and the extent of interaction between water, gases, and mineral surfaces, which, consequently, influences the composition of water arriving in groundwater and streams. The role of flow through weathered bedrock in controlling solute and nutrient loads in streams is often inferred via mixing models (34, 35), because direct measurements of fluid composition in unsaturated weathered bedrock within hillslopes (and dynamics) are challenging and rare (36, 37). At our site, the accumulation of successive early wet-season rains as rock moisture storage likely creates a geochemical mixing reservoir in the upper several meters of weathered bedrock. Oshun et al. (38) found that isotopic signatures (oxygen and hydrogen) of rainfall are rarely transmitted to groundwater, and groundwater isotopic concentrations are nearly constant and roughly equal to the average composition of rainfall. Furthermore, Kim et al. (13, 39) proposed that rapid cation exchange processes occurring in the zone of seasonal rock moisture storage control cation concentrations in groundwater during the wet season. Their high-frequency sampling of groundwater wells and streamflow in adjacent Elder Creek indicated that 43–74% of solute fluxes originated within the rock moisture zone (13). Kim et al. (39) also reported pCO_2 up to 8% at depths of 14 m. This suggests that the zone of seasonal rock moisture storage is an environment rich in diverse and seasonally dynamic microbial populations (40). Together, these findings imply that hydrogeochemical and reactive transport models concerned with understanding controls on stream solute fluxes need to explicitly treat rock moisture dynamics to account for the mixing and potentially rapid geochemical reactions occurring in weathered bedrock. Deep rock moisture dynamics may also influence biogeochemical cycling of carbon and nutrients, but with the exception of few detailed studies (41, 42), this remains relatively unexplored. Over the long term, feedbacks between atmospheric CO_2 and bedrock weathering are likely influenced by the dynamics of rock moisture storage. Therefore, this zone may require explicit treatment in models that seek to simulate interactions between biogeochemical cycles and the climate system (43).

The Influence of Rock Moisture on Vegetation and the Atmosphere. Rock moisture availability may control above-ground ecosystems by controlling the dominant vegetation. Our study site supports a

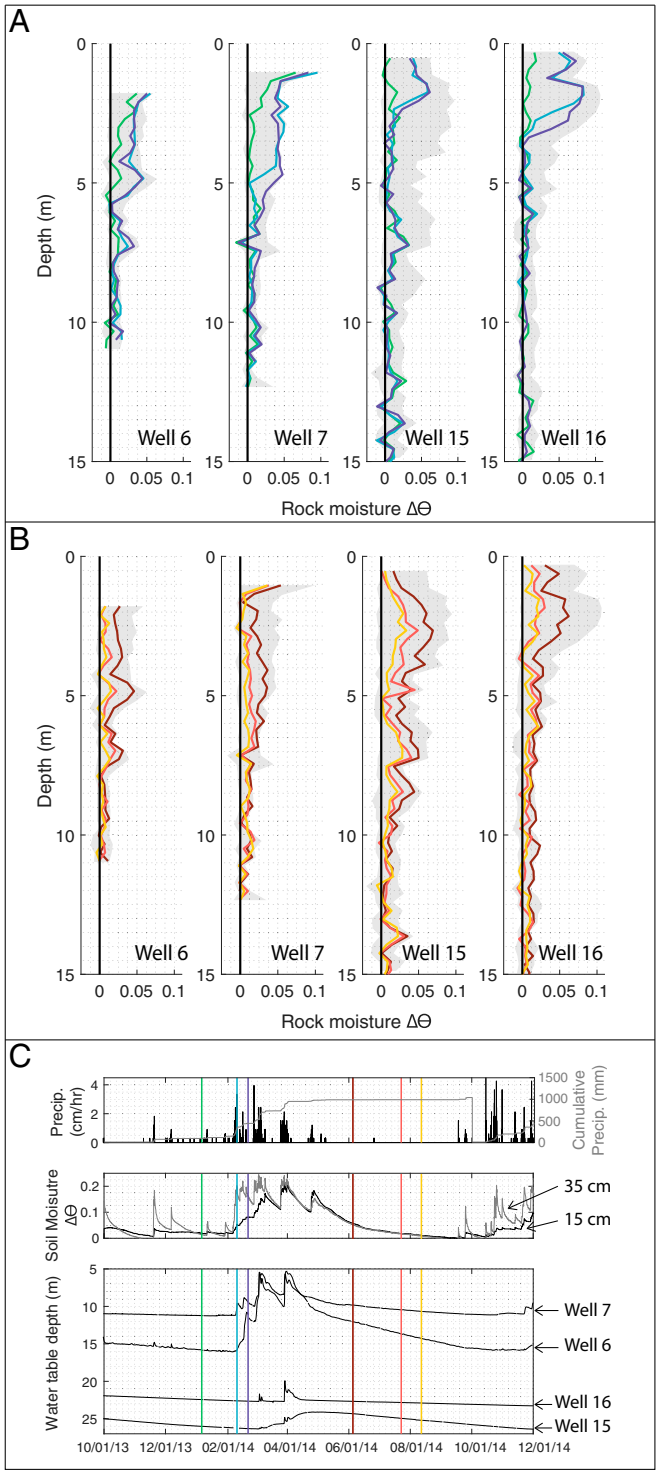

Fig. 3. Seasonal soil moisture, rock moisture, and groundwater dynamics: Vertical profiles of rock moisture change, $\Delta\theta$, illustrate that in the early wet-season, a wetting front progresses downward before the seasonal rise of the water table (*A*), while, during the dry season, rock moisture is progressively depleted (*B*), as groundwater recedes (*C*). Gray shading marks the total range of $\Delta\theta$ measured over the entire monitoring period (*Materials and Methods*). Colored lines in *A* and *B* correspond to the colored vertical lines marked in the precipitation, soil moisture, and groundwater level time series shown in *C*. Soil moisture dynamics at two depths near the ridge (15 and 35 cm) and groundwater dynamics in four wells are shown in *C*, *Middle* and *Bottom*. The locations of sensors and wells is shown in Fig. S1.

dense evergreen forest. Five consecutive years of severe drought in California led to the death of >100 million trees since 2010 (44), but we are aware of no drought-related tree mortality near our study site. The annual restocking of rock moisture even in dry years indicates that, so long as there is sufficient precipitation to reach maximum rock moisture storage annually, a consistent rock moisture reservoir will be available to vegetation each dry season. This suggests that understanding rock moisture storage availability and capacity should be considered in forecasting large-scale forest cover response to droughts and climate change.

Perhaps the most significant, and pressing, influence of rock moisture is through its influence on atmospheric circulation by regulating transpiration fluxes. We propose that inclusion of rock moisture dynamics is likely needed for accurate prediction of land–atmosphere exchange of water and energy in land-surface models (LSMs). Our field study demonstrated that dynamic rock moisture storage (much of which is transpired back to the atmosphere) can be 27% of the total annual precipitation. The rock moisture reservoir sustains late dry-season ET fluxes by direct tapping of stored moisture by tree roots and their symbiotes. Current models incorporated into LSMs rely on other mechanisms to provide water access to plants in the absence of rainfall, such as capillary flux from groundwater to the root zone (45–47). We note that there was no indication of upward capillary flux at our site. Instead, the slowly depleted reservoir of rock moisture was hosted within a 4- to 12-m-thick zone that was separated from a receding groundwater table by many meters of unsaturated fractured bedrock (Figs. 2 and 3).

Hydrologic models, including those used in LSMs, could alternatively model rock moisture storage as deep soil moisture in variably thick soils (48). There is no relationship, however, between soil thickness and the thickness of weathered bedrock hosting rock moisture, and the two material types likely require different model treatment. Preferential flow has been recognized for decades as a target for improvement in hydrological modeling (49–51), and our findings suggest that mechanistic understanding of this behavior is indeed needed to capture how weathered bedrock influences partitioning of precipitation between ET and runoff. For example, incorporation of transport phenomena associated with fracture flow (e.g., film flow; ref. 49) is likely needed to accurately simulate the simultaneous significant storage and rapid transmission of precipitation events after winter wet-up. Novel parameterizations of porous media flow for use in LSMs that account for processes in weathered bedrock are being developed (52–54). Such models present an opportunity to understand the role of rock moisture on the climate system.

Conclusion

Rock moisture, the exchangeable water stored in the matrix and fractures of weathered bedrock, is a significant, but not yet formally recognized, component of the terrestrial hydrologic cycle. The results of our intensive, direct monitoring across a hillslope reveal significant storage of rainfall as rock moisture. The rock moisture reservoir sustains dry-season transpiration and controls the timing, and likely geochemical composition, of runoff. Explicit treatment of this moisture reservoir is needed to predict hydrologic fluxes, particularly in simulating ecosystem response to droughts, as rock moisture can provide a hidden, but critical, water source to vegetation. Currently, no studies which systematically document rock moisture dynamics over large areas have been done, which makes incorporation of rock moisture into large-scale models problematic. However, several models have been recently proposed to predict the structure of the weathered bedrock region (23), and such models provide a means of identifying where rock moisture storage is likely to significantly impact hydrologic fluxes. There are few direct measurements of rock moisture that can be used to constrain rock moisture dynamics in hydrologic, climate, and reactive transport models. An increase in the number of direct measurements as well as improvements in

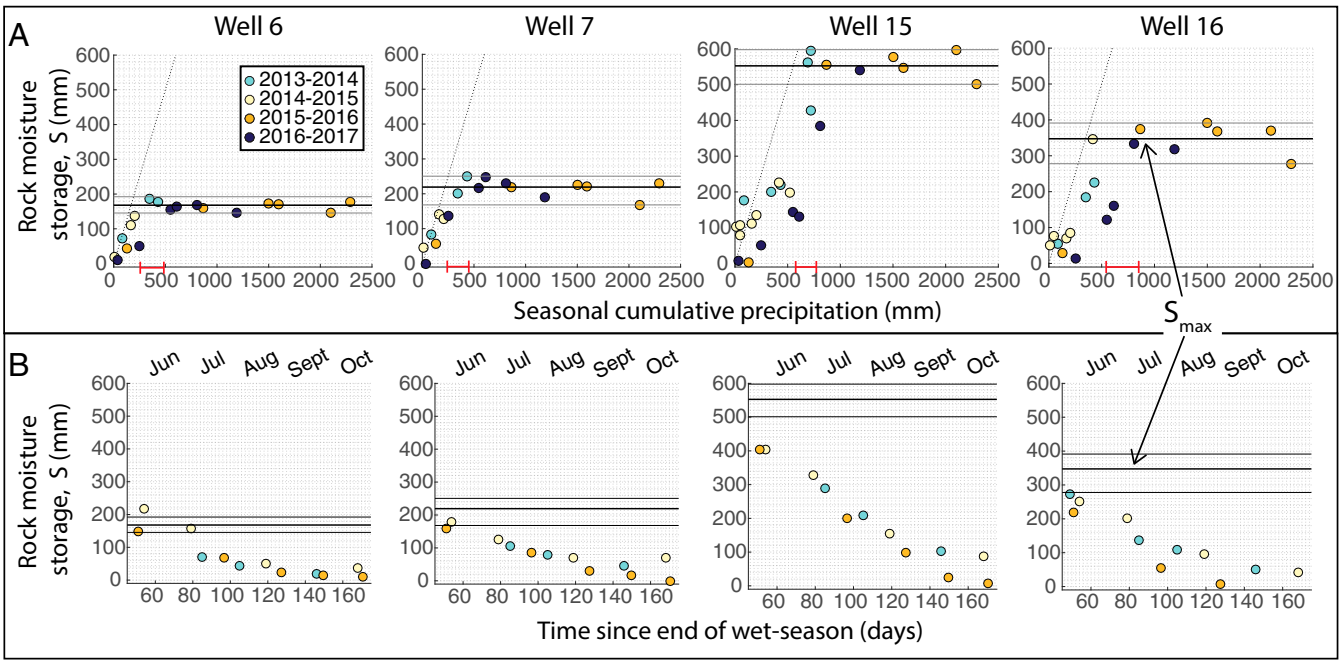

Fig. 4. Annually consistent patterns of rock moisture storage. (*A*) In different years (represented by different colors), rock moisture storage, *S* (mm), increases with increasing cumulative seasonal precipitation, until a maximum rock moisture (S_{max}) is reached (average and range are shown as thick and thin horizontal lines, respectively; Table S3). Thick red bars mark the range of precipitation when seasonal groundwater first responds at each well (Table S2). *S* is calculated for all depths that were above the water table at the time of measurement. (*B*) *S* declines following the final storm of the wet season. In years with different seasonal cumulative precipitation, the magnitude and timing of decline is roughly similar. The approximate month associated with the time since the end of the wet season is labeled. Other wells are shown in Figs. S3 and S4.

measurement techniques are needed. The combination of detailed rock moisture measurements in diverse environments and models for predicting subsurface structure could lead to a means of quantifying the significance of rock moisture as a reservoir to vegetation, and thus to the atmosphere, globally, as well as the role of water circulation in weathered bedrock on biogeochemical cycles.

Materials and Methods

Site Description. The study site (39.729 N, 123.644 W) is a steep (average 32°) 4,000-m^2 hillslope within the Northern California Coast Ranges that drains to the 17-km^2 catchment, Elder Creek at 392 m above sea level. The climate is characterized as Mediterranean, with warm dry summers and cool wet winters, with the vast majority of precipitation falling between October and May. The area receives an annual average of 2,042 mm of rain (55) with very little snow. The relatively dense forest is old growth needleleaf and broadleaf evergreen with a limited understory. Species include Douglas fir (*Pseudotsuga menziesii*), interior live oak (*Quercus wislizeni*), tanoak (*Notholithocarpus densiflorus*), Pacific madrone (*Arbutus menziesii*), and California bay (*Umbellularia californica*). Douglas fir forms the overstory at the site (Fig. 1), with heights up to 55–60 m. Active uplift in the region leads to erosion rates of ∼0.2–0.4 mm/y (56). The underlying geology, mapped as the Yager Terrane of the Coastal Belt of the Franciscan Formation (57), is a record of the accreted terrain of the North American plate margin and is described as well-bedded, little sheared, locally highly folded mudstone-rich turbidities with interbeds and lenses of sandstone and conglomerate (58). Most of the site is underlain by nearly vertically dipping argillite, which strikes approximately parallel to the hillslope gradient. Groundwater levels indicate that flow is directed across, rather than along, the bedding orientation. The pervasive fracturing likely prevents the bedding from controlling the groundwater flow direction. Along the eastern divide, a sandstone interbed is exposed at the surface (Fig. S1).

Hydrological Monitoring. As part of the Eel River Critical Zone Observatory, formerly Keck Hydrowatch, >750 sensors across Rivendell report nearly real-time hydrologic and climatological data (sensor.berkeley.edu). Groundwater wells were drilled in 2007 and 2010 (Fig. S1 and Table S2) and outfitted with submersible pressure transducers (CS450 and CS451; Campbell Scientific, Inc.) for monitoring of groundwater levels. Discharge in Elder Creek was measured at US Geological Survey Station 11475560 ∼150 m upstream of the site. Continuous measurements of soil were made via time-domain reflectometry (TDR) (*SI Materials and Methods* and Fig. S2), and precipitation was recorded by using a tipping bucket rain gauge (TE525; Campbell Scientific, Inc.) in a meadow directly across from the site. Further details can be found in Salve et al. (16).

Measurement of Rock Moisture Storage. Changes in rock moisture storage in space and time were measured via successive downhole neutron probe surveys (CPN 503DR Hydroprobe, serial no. 4340702152; Instrotek Inc.) in a network of nine wells (Fig. 1 and Fig. S1). Neutron probe counts, *N* (counts per 16 s), were measured in 0.3-m intervals within the unsaturated zone at various times over the period 2013–2016. Because *N* is directly proportional to volumetric water content, θ, and changes in *N* have been shown to accurately reflect successive changes in θ at a specific location over time (59), we used *N* to evaluate the timing and spatial pattern of rock moisture storage. The volume of rock moisture storage, *S* (millimeters), was estimated by using a linear relationship between *N* and θ developed by using a barrel calibration for the specific borehole casing materials and instrument used in this study (*SI Materials and Methods*). At each depth, Δθ was calculated as the difference between θ for that survey and a reference dry survey (October 25, 2015). To estimate *S*, discrete Δθ measurements were applied to each 0.3-m measurement interval and summed over all depth intervals between the soil and the location of the water table at the time of measurement. The uncertainty in Δθ accounting for instrument precision was 0.003 m^3/m^3. The uncertainty in the thickness over which Δθ applied was estimated as 0.02 m/m (*SI Materials and Methods*). This led to ∼2% uncertainty in values of *S*. The value S_{max} is the average *S* over the wet-season surveys which showed high Δθ throughout the entire profile (i.e., excluding surveys which showed evidence of progressive wetting or drying of the profile; Table S3).

ACKNOWLEDGMENTS. We thank Inez Fung, Todd Dawson, Jasper Oshun, W. Jesse Hahm, Rohit Salve, and the many students who contributed to field data collection. This work was supported by the Keck Foundation; National Science Foundation Grant EAR 1331940 (for the Eel River Critical Zone Observatory), and The University of California Reserve System. Lidar data were collected by the National Center for Airborne Laser Mapping.

1. Matthes JH, Goring S, Williams JW, Dietze MC (2016) Benchmarking historical CMIP5 plant functional types across the Upper Midwest and Northeastern United States. *J Geophys Res Biogeosci* 121:523–535.
2. Matheny AM, et al. (2014) Characterizing the diurnal patterns of errors in the prediction of evapotranspiration by several land-surface models: An NACP analysis. *J Geophys Res Biogeosci* 119:1458–1473.
3. McColl KA, et al. (2017) The global distribution and dynamics of surface soil moisture. *Nat Geosci* 10:100–104.
4. Ochsner TE, et al. (2013) State of the art in large-scale soil moisture monitoring. *Soil Sci Soc Am J* 77:1888–1919.
5. Fan Y, Miguez-Macho G, Jobbágy EG, Jackson RB, Otero-Casal C (2017) Hydrologic regulation of plant rooting depth. *Proc Natl Acad Sci USA* 114:10572–10577.
6. Salvucci GD, Entekhabi D (1995) Hillslope and climatic controls on hydrologic fluxes. *Water Resour Res* 31:1725–1739.
7. Koirala S, et al. (2017) Global distribution of groundwater-vegetation spatial covariation. *Geophys Res Lett* 44:4134–4142.
8. Graham RC, Rossi AM, Hubbert KR (2010) Rock to regolith conversion: Producing hospitable substrates for terrestrial ecosystems. *GSA Today* 20:4–9.
9. Schwinning S (2010) The ecohydrology of roots in rocks. *Ecohydrology* 3:238–245.
10. Zwieniecki MA, Newton M (1996) Seasonal pattern of water depletion from soil-rock profiles in a Mediterranean climate in southwestern Oregon. *Can J For Res* 26: 1346–1352.
11. Anderson SP, Dietrich WE, Brimhall GH (2002) Weathering profiles, mass-balance analysis, and rates of solute loss: Linkages between weathering and erosion in a small, steep catchment. *Geol Soc Am Bull* 114:1143–1158.
12. Banks EW, et al. (2009) Fractured bedrock and saprolite hydrogeologic controls on groundwater/surface-water interaction: A conceptual model (Australia). *Hydrogeol J* 17:1969–1989.
13. Kim H, Dietrich WE, Thurnhoffer BM, Bishop JK, Fung IY (2017) Controls on solute concentration-discharge relationships revealed by simultaneous hydrochemistry observations of hillslope runoff and stream flow: The importance of critical zone structure. *Water Resour Res* 53:1424–1443.
14. Taylor G, Eggleton RA (2001) *Regolith Geology and Geomorphology* (Wiley, New York).
15. Ollier C, Pain C (1996) *Regolith, Soils and Landforms* (John Wiley & Sons, New York).
16. Salve R, Rempe DM, Dietrich WE (2012) Rain, rock moisture dynamics, and the rapid response of perched groundwater in weathered, fractured argillite underlying a steep hillslope. *Water Resour Res,* 48:W11528.
17. Ireson AM, et al. (2006) Hydrological processes in the chalk unsaturated zone—Insights from an intensive field monitoring programme. *J Hydrol (Amst)* 330:29–43.
18. Rempe DM, Dietrich WE (2014) A bottom-up control on fresh-bedrock topography under landscapes. *Proc Natl Acad Sci USA* 111:6576–6581.
19. Link P, et al. (2014) Species differences in the seasonality of evergreen tree transpiration in a Mediterranean climate: Analysis of multiyear, half-hourly sap flow observations. *Water Resour Res* 50:1869–1894.
20. Wald JA, Graham RC, Schoeneberger PJ (2013) Distribution and properties of soft weathered bedrock at≤ 1 m depth in the contiguous United States. *Earth Surf Process Landf* 38:614–626.
21. Moon S, Perron JT, Martel SJ, Holbrook WS, St Clair J (2017) A model of three-dimensional topographic stresses with implications for bedrock fractures, surface processes, and landscape evolution. *J Geophys Res Earth Surf* 122:823–846.
22. Chou PY, et al. (2014) Characterising the spatial distribution of transmissivity in the mountainous region: Results from watersheds in central Taiwan. *Fractured Rock Hydrogeology* (CRC, Boca Raton, FL), pp 115–127.
23. Riebe CS, Hahm WJ, Brantley SL (2017) Controls on deep critical zone architecture: A historical review and four testable hypotheses. *Earth Surf Process Landf* 42:128–156.
24. Lebedeva MI, Brantley SL (2013) Exploring geochemical controls on weathering and erosion of convex hillslopes: Beyond the empirical regolith production function. *Earth Surf Process Landf* 38:1793–1807.
25. Soulsby C, et al. (2007) Inferring groundwater influences on surface water in montane catchments from hydrochemical surveys of springs and streamwaters. *J Hydrol (Amst)* 333:199–213.
26. Haria A, Shand P (2004) Evidence for deep sub-surface flow routing in forested upland Wales: Implications for contaminant transport and stream flow generation. *Hydrol Earth Syst Sci Discuss* 8:334–344.
27. Hale VC, McDonnell JJ (2016) Effect of bedrock permeability on stream base flow mean transit time scaling relations: 1. A multiscale catchment intercomparison. *Water Resour Res* 52:1358–1374.
28. Gabrielli CP, McDonnell JJ, Jarvis WT (2012) The role of bedrock groundwater in rainfall–runoff response at hillslope and catchment scales. *J Hydrol* 450–451:117–133.
29. Tromp-van Meerveld HJ, Peters NE, McDonnell JJ (2007) Effect of bedrock permeability on subsurface stormflow and the water balance of a trenched hillslope at the Panola Mountain Research Watershed, Georgia, USA. *Hydrol Processes* 21:750–769.
30. Shimojima E, et al. (2000) Using short-and long-term transients in seepage discharge and chemistry in a mountain tunnel to quantify fracture and matrix water fluxes. *J Hydrol (Amst)* 234:142–161.
31. Graham RC, et al. (1997) Morphology, porosity, and hydraulic conductivity of weathered granitic bedrock and overlying soils. *Soil Sci Soc Am J* 61:516–522.
32. Querejeta JI, Estrada-Medina H, Allen MF, Jiménez-Osornio JJ (2007) Water source partitioning among trees growing on shallow karst soils in a seasonally dry tropical climate. *Oecologia* 152:26–36.
33. Hasenmueller EA, et al. (2017) Weathering of rock to regolith: The activity of deep roots in bedrock fractures. *Geoderma* 300:11–31.
34. Mulholland PJ (1993) Hydrometric and stream chemistry evidence of three storm flowpaths in Walker Branch Watershed. *J Hydrol* 151:291–316.
35. Genereux DP, Hemond HF (1990) Three-component tracer model for stormflow on a small Appalachian forested catchment—Comment. *J Hydrol* 117:377–380.
36. Geake AK, Foster SSD (1989) Sequential isotope and solute profiling in the unsaturated zone of British Chalk. *Hydrol Sci J* 34:79–95.
37. Jardine PM, et al. (2002) Influence of hydrological and geochemical processes on the transport of chelated metals and chromate in fractured shale bedrock. *J Contam Hydrol* 55:137–159.
38. Oshun J, Dietrich WE, Dawson TE, Fung I (2016) Dynamic, structured heterogeneity of water isotopes inside hillslopes. *Water Resour Res* 52:164–189.
39. Kim H, Bishop JK, Dietrich WE, Fung IY (2014) Process dominance shift in solute chemistry as revealed by long-term high-frequency water chemistry observations of groundwater flowing through weathered argillite underlying a steep forested hillslope. *Geochim Cosmochim Acta* 140:1–19.
40. McMahon MJ, Christy AD (2000) Root growth, calcite precipitation, and gas and water movement in fractures and macropores: A review with field observations. *Ohio J Sci* 100:88–93.
41. Jardine PM, et al. (2006) Vadose zone flow and transport of dissolved organic carbon at multiple scales in humid regimes. *Vadose Zone J* 5:140–152.
42. Buss HL, Mathur R, White AF, Brantley SL (2010) Phosphorus and iron cycling in deep saprolite, Luquillo Mountains, Puerto Rico. *Chem Geol* 269:52–61.
43. Doughty CE, Taylor LL, Girardin CAJ, Malhi Y, Beerling DJ (2014) Montane forest root growth and soil organic layer depth as potential factors stabilizing Cenozoic global change. *Geophys Res Lett* 41:983–990.
44. US Department of Agriculture (2016) *New Aerial Survey Identifies More than 100 Million Dead Trees in California* (US Department of Agriculture, Vallejo, CA).
45. Miguez-Macho G, Fan Y (2012) The role of groundwater in the Amazon water cycle: 2. Influence on seasonal soil moisture and evapotranspiration. *J Geophys Res D Atmospheres* 117:D15.
46. Lam HA, Karssenberg DJ, Van den Hurk BJJM, Bierkens MFP (2011) Spatial and temporal connections in groundwater contribution to evaporation. *Hydrol Earth Syst Sci* 15:2621–2630.
47. Fan Y, Miguez-Macho G, Weaver CP, Walko R, Robock A (2007) Incorporating water table dynamics in climate modeling: 1. Water table observations and equilibrium water table simulations. *J Geophys Res* 112:D10125.
48. Brunke MA, et al. (2016) Implementing and evaluating variable soil thickness in the community land model, version 4.5 (CLM4. 5). *J Clim* 29:3441–3461.
49. Tokunaga TK, Wan J (1997) Water film flow along fracture surfaces of porous rock. *Water Resour Res* 33:1287–1295.
50. Nimmo JR (2010) Theory for source-responsive and free-surface film modeling of unsaturated flow. *Vadose Zone J* 9:295–306.
51. Neuman SP (2005) Trends, prospects and challenges in quantifying flow and transport through fractured rocks. *Hydrogeol J* 13:124–147.
52. Vrettas MD, Fung IY (2015) Toward a new parameterization of hydraulic conductivity in climate models: Simulation of rapid groundwater fluctuations in Northern California. *J Adv Model Earth Syst* 7:2105–2135.
53. Vrettas MD, Fung IY (2017) Sensitivity of transpiration to subsurface properties: Exploration with a 1-D model. *J Adv Model Earth Syst* 9:1030–1045.
54. Ireson AM, van der Kamp G, Nachshon U, Butler AP (2013) Modeling groundwater-soil-plant-atmosphere exchanges in fractured porous media. *Procedia Environ Sci* 19: 321–330.
55. PRISM Climate Group (2017) PRISM Climate Data. Available at prism.oregonstate.edu. Accessed February 15, 2018.
56. Fuller TK, Perg LA, Willenbring JK, Lepper K (2009) Field evidence for climate-driven changes in sediment supply leading to strath terrace formation. *Geology* 37:467–470.
57. McLaughlin RJ, et al. (2000) Geology of the cape Mendocino, Eureka, Garberville, and southwestern part of the Hayfork 30 × 60 minute quadrangles and adjacent offshore area, northern California, Miscellaneous Field Studies Map (US Geological Survey, Washington, DC), MF-2336.
58. Blake MC, Jr, Jayko AS, McLaughlin RJ (1985) Tectonostratigraphic terranes of northern California. *Tectonostratigraphic Terranes of the Circum-Pacific Region*, Earth Science Series, ed Howell DG (Circumpacific Council for Energy and Mineral Resources, Houston), Vol 1, pp 159–171.
59. Long I, French B (1967) Measurement of soil moisture in the field by neutron moderation. *J Soil Sci* 18:149–166.